

# Acidic Salts of the Decaoxidoperiodic Acid: $\text{NiH}_4\text{I}_2\text{O}_{10} \cdot 6\text{H}_2\text{O}$ , $\text{ZnH}_4\text{I}_2\text{O}_{10} \cdot 6\text{H}_2\text{O}$ and $\text{MgH}_4\text{I}_2\text{O}_{10} \cdot 6\text{H}_2\text{O}$ ; Crystal Structures, Vibrational Spectra and Thermal Decomposition

Margarita Aleksandrova<sup>a</sup>, Hartmut Haeuseler<sup>a</sup>, Ralph Jaquet<sup>b</sup>, and Michael Wagener<sup>a</sup>

<sup>a</sup> Laboratorium für Anorganische Chemie der Universität Siegen, D-57068 Siegen, Germany

<sup>b</sup> Theoretische Chemie der Universität Siegen, D-57068 Siegen, Germany

Reprint requests to Prof. Dr. H. Haeuseler. Fax: ++49 271 740 2555.

E-mail: haeuseler@chemie.uni-siegen.de

Z. Naturforsch. 2008, 63b, 1367–1376; received September 9, 2008

By crystallization from strongly acidic aqueous solutions, nickel and zinc tetrahydrogen-decaoxodiperiodate hexahydrate,  $\text{NiH}_4\text{I}_2\text{O}_{10} \cdot 6\text{H}_2\text{O}$  and  $\text{ZnH}_4\text{I}_2\text{O}_{10} \cdot 6\text{H}_2\text{O}$ , have been obtained and found to be isotypic to  $\text{CuH}_4\text{I}_2\text{O}_{10} \cdot 6\text{H}_2\text{O}$  ( $P2_1/c$ , no. 14) with the lattice parameters  $a = 1070.3$ ,  $b = 544.0$ ,  $c = 1187.2$  pm,  $\beta = 112.6^\circ$  for the Ni compound and  $a = 1073.3$ ,  $b = 545.3$ ,  $c = 1189.5$  pm and  $\beta = 112.5^\circ$  for the Zn compound. The crystal structure of  $\text{MgH}_4\text{I}_2\text{O}_{10} \cdot 6\text{H}_2\text{O}$  has been reinvestigated and contrary to former results found to be isotypic to the Cu compound as well. IR and Raman spectra are given and analyzed with respect to the internal vibrations of the  $\text{H}_4\text{I}_2\text{O}_{10}^{2-}$  ion and the hydrogen bonding system. According to high-temperature Raman spectra and DTA and TG measurements, the compounds decompose in the temperature range up to 300 °C via unknown salts with the anions  $\text{H}_4\text{IO}_6^{2-}$  and  $\text{IO}_4^-$  to the corresponding iodates. In the case of the Ni compound the exothermic decomposition to the iodate occurs in two steps.

**Key words:** Periodate, Crystal Structure, Vibrational Spectroscopy, Thermal Analysis

## Introduction

In the literature only very few data can be found on periodates with the anion  $\text{H}_4\text{I}_2\text{O}_{10}^{2-}$ . The first tetrahydrogendecaoxidoperiodate,  $\text{Li}_2\text{H}_4\text{I}_2\text{O}_{10}$ , was obtained in 1996 by Jansen and Müller [1] by dehydration of  $\text{LiH}_4\text{IO}_6 \cdot \text{H}_2\text{O}$  at 83 °C. Some years later Nagel *et al.* [2] were successful in preparing  $\text{MgH}_4\text{I}_2\text{O}_{10} \cdot 6\text{H}_2\text{O}$  from a strongly acidic ( $\text{pH} < 1$ ) solution by reaction of a 30 % solution of periodic acid with basic magnesium carbonate. In the same paper the existence of a presumably isotypic  $\text{ZnH}_4\text{I}_2\text{O}_{10} \cdot 6\text{H}_2\text{O}$  has been reported. According to [2],  $\text{MgH}_4\text{I}_2\text{O}_{10} \cdot 6\text{H}_2\text{O}$  crystallizes monoclinically in space group  $P2_1$ , but in the ICSD data base besides the structure with space group  $P2_1$  an averaged structure with space group  $P2_1/c$  is recorded also citing the same original paper of Nagel *et al.* [2]. Therefore we decided to reinvestigate the structure of  $\text{MgH}_4\text{I}_2\text{O}_{10} \cdot 6\text{H}_2\text{O}$  and to investigate that of the corresponding Zn compound.

In the course of this study we have been looking also for Ni periodates. According to the lit-

erature, in the system NiO-H<sub>2</sub>O-I<sub>2</sub>O<sub>7</sub> there exist only two compounds: Zhang *et al.* [3] reported on  $\text{NiH}_3\text{IO}_6 \cdot 6\text{H}_2\text{O}$  and Nabar and Athawale [4] described the compound  $\text{Ni}_2\text{HIO}_6 \cdot 3\text{H}_2\text{O}$ . Of these two compounds the trihydrogenhexaoxoperiodate has been investigated by X-ray diffraction methods and by vibrational spectroscopy while  $\text{Ni}_2\text{HIO}_6 \cdot 3\text{H}_2\text{O}$  has been characterized by thermoanalysis only. Ni salts of the diperiodic acid  $\text{H}_6\text{I}_2\text{O}_{10}$  have not been known until now.

The vibrational spectra of the different decaoxodiperiodate ions are not well known. There are only three papers in the literature [2, 4, 5] dealing with the IR and Raman spectra of the diperiodate ion and the assignment of its internal vibrations. Recently we have published a vibrational analysis of the  $\text{H}_4\text{I}_2\text{O}_{10}^{2-}$  ion including quantum chemical calculations [6] in which we found that the Raman lines and IR absorptions with the highest wavenumbers in the range below 1000  $\text{cm}^{-1}$  are due to torsional vibrations of the I-OH groups and not due to the terminal I-O bonds of the ion as claimed in earlier papers.

	1	2	3
Formula	ZnH <sub>4</sub> I <sub>2</sub> O <sub>10</sub> · 6H <sub>2</sub> O	NiH <sub>4</sub> I <sub>2</sub> O <sub>10</sub> · 6H <sub>2</sub> O	MgH <sub>4</sub> I <sub>2</sub> O <sub>10</sub> · 6H <sub>2</sub> O
<i>M<sub>r</sub></i>	591.3	584.64	550.24
Cryst. size, mm <sup>3</sup>	0.11 × 0.07 × 0.08	0.14 × 0.1 × 0.04	0.14 × 0.06 × 0.02
Crystal system	monoclinic	monoclinic	monoclinic
Space group	<i>P</i> 2 <sub>1</sub> / <i>c</i> (no. 14)	<i>P</i> 2 <sub>1</sub> / <i>c</i> (no. 14)	<i>P</i> 2 <sub>1</sub> / <i>c</i> (no. 14)
<i>a</i> , pm	1073.8(2)	1070.3(2)	1071.5(2)
<i>b</i> , pm	546.29(11)	543.30(10)	547.10(10)
<i>c</i> , pm	1189.5(2)	1187.2(2)	1194.9(2)
β, deg	112.52(3)	112.55(3)	112.53(3)
<i>V</i> , Å <sup>3</sup>	644.6(2)	637.6(2)	647.0(2)
<i>Z</i>	2	2	2
<i>D</i> <sub>calcd</sub> , g cm <sup>-3</sup>	3.05	3.05	2.82
μ(MoK <sub>α</sub> ), cm <sup>-1</sup>	6.780	6.449	4.994
<i>F</i> (000), e	560	556	524
<i>hkl</i> range	-15 ≤ <i>h</i> ≤ +15 -8 ≤ <i>k</i> ≤ +8 -17 ≤ <i>l</i> ≤ +17	-15 ≤ <i>h</i> ≤ +15 -7 ≤ <i>k</i> ≤ +7 -16 ≤ <i>l</i> ≤ +16	-15 ≤ <i>h</i> ≤ +15 -7 ≤ <i>k</i> ≤ +7 -17 ≤ <i>l</i> ≤ +16
(( <i>sinθ</i> )/λ) <sub>max</sub> , Å <sup>-1</sup>	0.738	0.712	0.713
Refl. measured	8936	7211	7329
Refl. unique	2139	1926	1852
<i>R</i> <sub>int</sub>	0.0685	0.0324	0.0426
Param. refined	113	113	112
<i>R</i> ( <i>F</i> )/ <i>wR</i> ( <i>F</i> <sup>2</sup> ) <sup>a</sup> (all refl.)	0.0364/0.0595	0.0305/0.0479	0.0359/0.566
GoF ( <i>F</i> <sup>2</sup> ) <sup>a</sup>	1.020	0.977	0.953
Δρ <sub>fin</sub> (max/min), e Å <sup>-3</sup>	1.21/-1.36	1.19/-0.95	0.77/-1.44

Table 1. Crystal data and data for the structure determination of ZnH<sub>4</sub>I<sub>2</sub>O<sub>10</sub> · 6H<sub>2</sub>O (1), NiH<sub>4</sub>I<sub>2</sub>O<sub>10</sub> · 6H<sub>2</sub>O (2), and MgH<sub>4</sub>I<sub>2</sub>O<sub>10</sub> · 6H<sub>2</sub>O (3).

<sup>a</sup> For the definition of *R* values and GoF, as well as the weighting scheme applied see the manual for SHELXL-97.

## Results and Discussion

The crystal structures of MgH<sub>4</sub>I<sub>2</sub>O<sub>10</sub> · 6H<sub>2</sub>O, NiH<sub>4</sub>I<sub>2</sub>O<sub>10</sub> · 6H<sub>2</sub>O, and ZnH<sub>4</sub>I<sub>2</sub>O<sub>10</sub> · 6H<sub>2</sub>O

All three compounds crystallize in the monoclinic space group *P*2<sub>1</sub>/*c* (no. 14), isotypic to CuH<sub>4</sub>I<sub>2</sub>O<sub>10</sub> · 6H<sub>2</sub>O [5]. Details of the structural analysis are given in Table 1. The structures were refined to *R*<sub>1</sub> < 2.5 and *wR*<sub>2</sub> < 5.7 %. Selected bond lengths and angles are given in Table 2.

As our reinvestigation of the crystal structure of MgH<sub>4</sub>I<sub>2</sub>O<sub>10</sub> · 6H<sub>2</sub>O shows, this compound does not crystallize in a structure of space group *P*2<sub>1</sub> as claimed by Nagel *et al.* [2] but is isotypic to the corresponding copper compound CuH<sub>4</sub>I<sub>2</sub>O<sub>10</sub> · 6H<sub>2</sub>O [5]. For the compounds NiH<sub>4</sub>I<sub>2</sub>O<sub>10</sub> · 6H<sub>2</sub>O and ZnH<sub>4</sub>I<sub>2</sub>O<sub>10</sub> · 6H<sub>2</sub>O we also found structures isotypic to CuH<sub>4</sub>I<sub>2</sub>O<sub>10</sub> · 6H<sub>2</sub>O as already suggested by the nearly identical lattice parameters and the great similarity of the vibrational spectra of all these compounds.

The structure is built from (100) layers of [M(H<sub>2</sub>O)<sub>6</sub>]<sup>2+</sup> octahedra (*M* = Mg, Zn, Cu, Ni) connected to layers formed by H<sub>4</sub>I<sub>2</sub>O<sub>10</sub><sup>2-</sup> ions *via* hydrogen bonds. The layers of the [M(H<sub>2</sub>O)<sub>6</sub>]<sup>2+</sup> octahedra consist of chains of octahedra linked to each other by hydrogen bonds OW2–H22···OW1 (see Fig. 1) running parallel to the *b* axis. All the other hydrogen

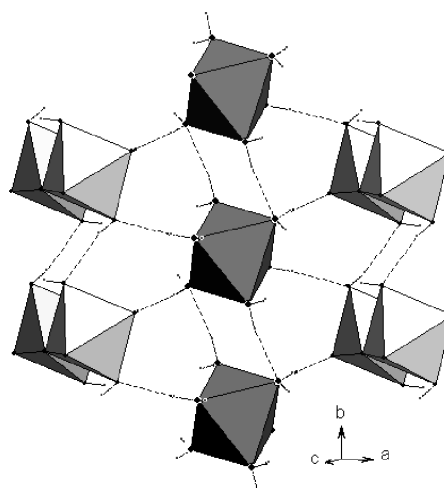


Fig. 1. Hydrogen bonds within a chain of [M(H<sub>2</sub>O)<sub>6</sub>]<sup>2+</sup> octahedra and the hydrogen bond system to the neighboring periodate ions.

atoms of the water molecules form hydrogen bonds to the periodate ions. So there is no direct connection between the chains of octahedra *via* hydrogen bonds. The diperiodate ions on the other hand are interconnected by hydrogen bonds O1–H1···O2 to form chains in the direction of the *b* axis and by hydrogen bonds O2–H2···O3 between these chains to form layers parallel to (100) (see Fig. 2).

Table 2. Selected distances (pm) and angles (deg) in  $\text{ZnH}_4\text{I}_2\text{O}_{10}\cdot 6\text{H}_2\text{O}$ ,  $\text{NiH}_4\text{I}_2\text{O}_{10}\cdot 6\text{H}_2\text{O}$ , and  $\text{MgH}_4\text{I}_2\text{O}_{10}\cdot 6\text{H}_2\text{O}$ .

Distances	<i>M</i> = Zn	<i>M</i> = Ni	<i>M</i> = Mg	Angles	<i>M</i> = Zn	<i>M</i> = Ni	<i>M</i> = Mg
<i>MO</i> <sub>6</sub> Octahedron							
<i>M</i> –OW1	206.9(2)	204.5(2)	206.1(3)	OW1– <i>M</i> –OW1	180	180	180
<i>M</i> –OW2	211.6(3)	206.7(2)	208.2(3)	OW1– <i>M</i> –OW3	87.4(1)	87.03(11)	87.96(13)
<i>M</i> –OW3	207.0(2)	203.9(2)	205.0(3)	OW1– <i>M</i> –OW2	92.6(1)	92.97(11)	92.04(13)
				OW1– <i>M</i> –OW2	91.6(1)	92.30(10)	90.88(13)
				OW2– <i>M</i> –OW2	180	180	180
				OW2– <i>M</i> –OW3	88.8(1)	88.96(12)	89.19(15)
				OW2– <i>M</i> –OW3	91.2(1)	91.04(12)	90.81(15)
				OW3– <i>M</i> –OW3	180	180	180
<i>H</i> <sub>4</sub> <i>I</i> <sub>2</sub> <i>O</i> <sub>10</sub> <sup>2−</sup> Ion							
I–O1(2)	190.1(2)	189.9(2)	190.2(3)	O1–I–O5	90.20(11)	90.12(9)	90.20(12)
I–O2(4)	190.9(2)	190.4(2)	190.9(3)	O1–I–O5	88.31(10)	88.14(10)	88.40(12)
I–O3(1)	181.1(2)	180.8(2)	180.7(2)	O2–I–O1	174.59(11)	174.39(10)	174.52(12)
I–O4(3)	178.6(2)	178.90(19)	179.2(2)	O2–I–O5	90.15(10)	90.17(9)	89.87(12)
I–O5	195.8(2)	195.87(19)	195.9(2)	O2–I–O5	86.51(10)	86.47(10)	86.29(12)
I–O5′	199.0(2)	199.00(19)	198.6(2)	O3–I–O1	92.53(12)	92.66(11)	92.71(14)
I–I′	309.41(13)	309.57(13)	309.60(13)	O3–I–O2	92.86(11)	92.93(11)	92.76(13)
				O3–I–O5	91.19(11)	91.40(9)	91.53(11)
				O3–I–O5′	167.95(10)	168.13(8)	168.07(10)
				O4–I–O1	89.47(11)	89.45(10)	89.41(13)
				O4–I–O2	88.92(11)	88.97(10)	89.23(13)
				O4–I–O3	102.36(11)	101.85(10)	102.25(12)
				O4–I–O5	166.45(10)	166.75(9)	166.21(11)
				O4–I–O5	89.66(10)	90.00(9)	89.63(11)
				O5–I–O5′	76.79(9)	76.75(9)	76.58(10)

Symmetry code for O5′ and I′:  $-x+1, -y, -z+1$ .

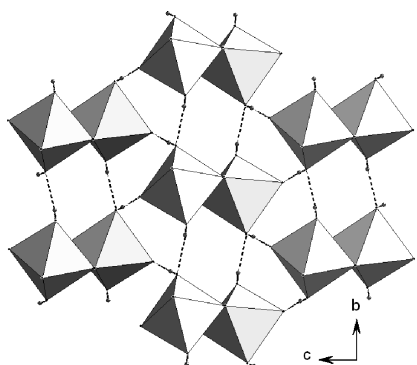


Fig. 2. Hydrogen bonds between the periodate ions within the layers parallel to (100).

Contrary to the  $[\text{Cu}(\text{H}_2\text{O})_6]^{2+}$  octahedra which show a strong Jahn-Teller distortion [5], all the  $[\text{M}(\text{H}_2\text{O})_6]^{2+}$  octahedra in the compounds reported in this paper are nearly ideal (see Table 2), but still the distances OW2–*M* which are longest in the Cu compound are slightly longer than the distances OW1–*M* and OW3–*M*. The angles between *cis*-standing water molecules are found in the range  $93^\circ$ – $87.7^\circ$  with the strongest deviation from the ideal value in the case of the Ni compound.

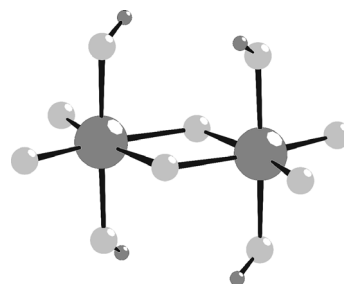


Fig. 3. Structure of the diperiodate ion  $\text{H}_4\text{I}_2\text{O}_{10}^{2-}$ .

The structure of the  $\text{H}_4\text{I}_2\text{O}_{10}^{2-}$  ion (see Fig. 3) is nearly unaffected by the nature of the metal ion. All distances and angles within the diperiodate ions remain the same within a very narrow range (see Table 2).

#### Vibrational spectroscopy

As  $\text{NiH}_4\text{I}_2\text{O}_{10}\cdot 6\text{H}_2\text{O}$  and  $\text{ZnH}_4\text{I}_2\text{O}_{10}\cdot 6\text{H}_2\text{O}$  react with KBr and CsI even in a Nujol mull, we could not obtain IR spectra of sufficient quality in the region of the internal vibrations of the  $\text{H}_4\text{I}_2\text{O}_{10}^{2-}$  ions. Therefore the IR spectra were recorded with a MIRacle-ATR unit on a Bruker FTIR instrument Tensor 27 in the range  $4000$ – $600\text{ cm}^{-1}$  and with a Bruker IFS 113v on

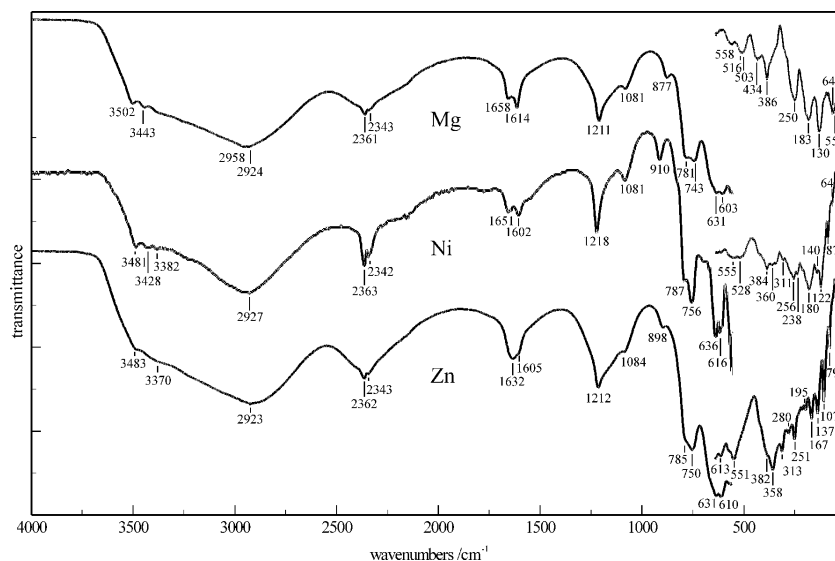


Fig. 4. IR spectra of  $\text{MgH}_4\text{I}_2\text{O}_{10} \cdot 6\text{H}_2\text{O}$ ,  $\text{NiH}_4\text{I}_2\text{O}_{10} \cdot 6\text{H}_2\text{O}$ ,  $\text{ZnH}_4\text{I}_2\text{O}_{10} \cdot 6\text{H}_2\text{O}$  ( $4000 - 600 \text{ cm}^{-1}$ : MIRacle ATR;  $650 - 50 \text{ cm}^{-1}$ : Nujol mull on polyethylene; the bands at  $2362$  and  $2343 \text{ cm}^{-1}$  are due to atmospheric  $\text{CO}_2$ ).

Nujol mulls on polyethylene disks in the range  $650 - 50 \text{ cm}^{-1}$  (Fig. 4).

Raman spectra of  $\text{NiH}_4\text{I}_2\text{O}_{10} \cdot 6\text{H}_2\text{O}$  and  $\text{ZnH}_4\text{I}_2\text{O}_{10} \cdot 6\text{H}_2\text{O}$  are shown in Fig. 5 for the region of the internal vibrations of the  $\text{H}_4\text{I}_2\text{O}_{10}^{2-}$  ions and the librational modes of the water molecules. For the Raman spectrum of  $\text{MgH}_4\text{I}_2\text{O}_{10} \cdot 6\text{H}_2\text{O}$  which is very similar to the spectra of the Ni and Zn compounds see [2].

During the measurement of the Raman spectra of  $\text{NiH}_4\text{I}_2\text{O}_{10} \cdot 6\text{H}_2\text{O}$  excited by a Nd:YAG laser ( $\lambda =$

$1064 \text{ nm}$ ) we found that this compound decomposes if the measurement is done with a too high power of the laser due to a local warming of the sample in the focus of the laser beam. But with a laser power below  $18 \text{ mW}$  a spectrum could be obtained without any sign of decomposition.

#### Internal vibrations of the $\text{H}_4\text{I}_2\text{O}_{10}^{2-}$ ions

In the region of the internal vibrations of the  $\text{H}_4\text{I}_2\text{O}_{10}^{2-}$  ions 4 maxima are observed (Fig. 5) analogous to the spectrum of  $\text{MgH}_4\text{I}_2\text{O}_{10} \cdot 6\text{H}_2\text{O}$  (compare Nagel *et al.* [2]) in the Raman spectra and 7 absorption peaks in the IR spectra (Fig. 4). Based on the results of the recently published *ab initio* calculations on the density functional level (B3LYP, BP86) of the vibrational frequencies of the  $\text{H}_4\text{I}_2\text{O}_{10}^{2-}$  ion [6], we assign the two IR maxima at  $1211$  and  $1081 \text{ cm}^{-1}$  (Mg),  $1218$  and  $1081 \text{ cm}^{-1}$  (Ni) and  $1212$  and  $1084 \text{ cm}^{-1}$  (Zn) to the deformation vibrations of the I–O–H groups [ $\nu(\text{IOH})$ ]. The corresponding Raman-active vibrations are not observed. The IR maxima at  $877$  and  $781$  (Mg),  $910$  and  $787$  (Ni), and  $898$  and  $785$  (Zn)  $\text{cm}^{-1}$  as well as the Raman lines at  $813$ ,  $762$  and  $756$  (Mg),  $816$ ,  $187$  and  $756$  (Ni) and  $816$ ,  $785$  and  $750$  (Zn)  $\text{cm}^{-1}$ , we assign to the torsional vibrations of the I–O–H groups. The stretching vibrations of the terminal I–O bonds [ $\nu(\text{IOt})$ ] are observed below  $650 \text{ cm}^{-1}$  both in the Raman and IR spectra. The symmetrical stretching vibration of the  $\text{I}(\text{OH})_2$  groups are found in the IR spectra at  $558$  (Mg),  $555$  (Ni) and  $551$  (Zn)  $\text{cm}^{-1}$ . The

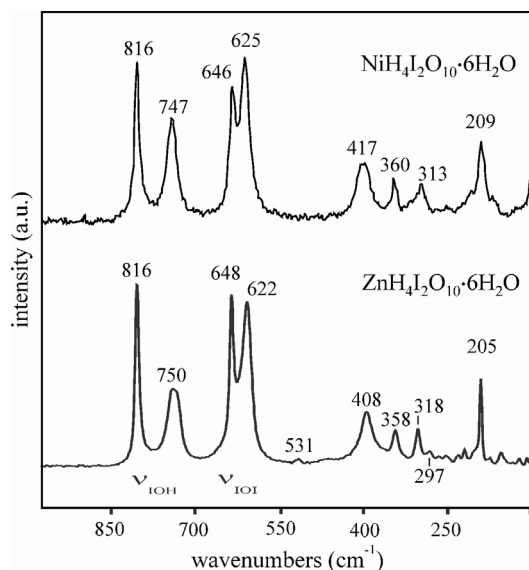


Fig. 5. Raman spectra of  $\text{NiH}_4\text{I}_2\text{O}_{10} \cdot 6\text{H}_2\text{O}$  and  $\text{ZnH}_4\text{I}_2\text{O}_{10} \cdot 6\text{H}_2\text{O}$  (for the spectrum of  $\text{MgH}_4\text{I}_2\text{O}_{10} \cdot 6\text{H}_2\text{O}$  see [2]).

Activity	Calculated		Experimental (Figs. 4 and 5)		
	Wavenumber (cm <sup>-1</sup> )	Assignment	Mg [2]	Ni	Zn
Ra	1344	IO-H deformation			
IR	1338	IO-H deformation	1211	1218	1212
Ra	1194	IO-H deformation			
IR	1191	IO-H deformation	1081	1081	1084
Ra	942	I-OH torsion sym	813	816	816
IR	930	I-OH torsion asym	877	910	898
IR / Ra	836	I-OH torsion sym	781 / 762	787	785
IR / Ra	832	I-OH torsion asym	743 / 746 <sup>a</sup>	756 / 747	750 / 750
Ra	670	I-O terminal sym	647	646	648
IR	664	I-O terminal asym	631	636	631
Ra	649	I-O terminal sym	618	625	622
IR	643	I-O terminal asym	603	616	610
IR	592	HO-I-OH sym	558	555	551
Ra	558	HO-I-OH + I-O-I sym	510	528	

Table 3. Calculated vibrational frequencies (cm<sup>-1</sup>) of the anion H<sub>4</sub>I<sub>2</sub>O<sub>10</sub><sup>2-</sup> in CuH<sub>4</sub>I<sub>2</sub>O<sub>10</sub> · 6H<sub>2</sub>O [6] and their assignment to the internal vibrations of the H<sub>4</sub>I<sub>2</sub>O<sub>10</sub><sup>2-</sup> ion in ZnH<sub>4</sub>I<sub>2</sub>O<sub>10</sub> · 6H<sub>2</sub>O, NiH<sub>4</sub>I<sub>2</sub>O<sub>10</sub> · 6H<sub>2</sub>O, and MgH<sub>4</sub>I<sub>2</sub>O<sub>10</sub> · 6H<sub>2</sub>O.

<sup>a</sup> low-temperature measurement.

corresponding Raman-active vibration is strongly coupled to the symmetrical I-O stretching vibration of the bridging oxygen atoms. A compilation of these assignments in comparison to the calculated frequencies of the H<sub>4</sub>I<sub>2</sub>O<sub>10</sub><sup>2-</sup> ion [6] is shown in Table 3.

Unequivocal assignments of the deformation vibrations of the periodate ion which are strongly coupled to some of the I-O stretching modes and to librational modes of the water molecules as well as of the stretching and deformation vibrations of the [M(H<sub>2</sub>O)<sub>6</sub>]<sup>2+</sup> octahedra are not possible due to the large number of possible vibrations.

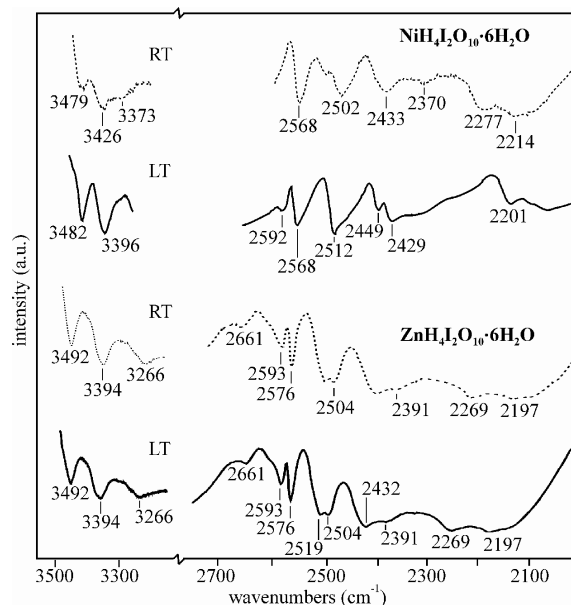


Fig. 6. Room-temperature (RT) and low-temperature (LT, liquid nitrogen) IR spectra of partially deuterated samples of NiH<sub>4</sub>I<sub>2</sub>O<sub>10</sub> · 6H<sub>2</sub>O and ZnH<sub>4</sub>I<sub>2</sub>O<sub>10</sub> · 6H<sub>2</sub>O (Nujol mull on CaF<sub>2</sub> windows).

### Hydrogen bonds

The IR-active stretching vibrations of the water of crystallization are found for all three compounds between 3500 and 2900 cm<sup>-1</sup> due to hydrogen bonds of different strength. Accordingly, the OD stretching vibrations of matrix isolated samples with HDO molecules are found between 2660 and 2130 cm<sup>-1</sup> as can be seen from Fig. 6. In Table 4 a tentative assignment of the wavenumbers of the OD stretching vibrations  $\nu(\text{OD})$  obtained from the low temperature spectra of isotopically dilute samples to the O...O distances obtained from the structure data is given together with the O...O distances calculated from these frequencies

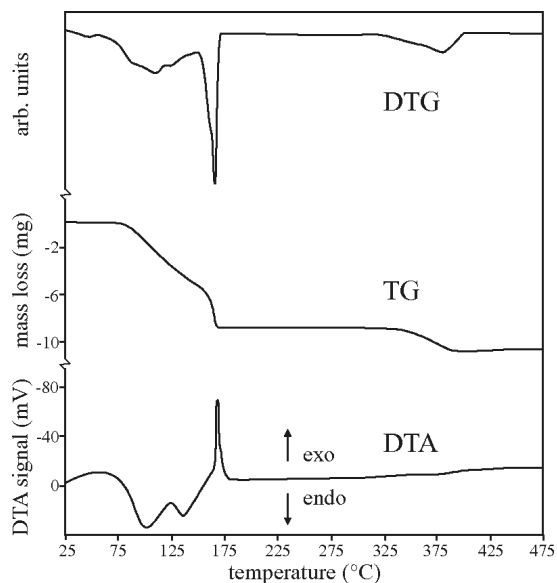


Fig. 7. Differential thermal analysis (DTA), thermogravimetric analysis (TG) and differential TG (DTG) of ZnH<sub>4</sub>I<sub>2</sub>O<sub>10</sub> · 6H<sub>2</sub>O.

	Donator D	H Atom	Acceptor A	$r_{DA}$	$\langle DHA \rangle$	$\nu(OH)$	$\nu(OD)$ (90 K)	$r_{DA}(\text{calcd.})$
Mg	OW1	H11	O3	281.6(4)	152(5)		2585	297.4
	OW1	H12	O4	264.6(4)	177(6)	2958	2397	271.3
	OW2	H21	O3	278.1(4)	160(6)		2456	277.4
	OW2	H22	OW1	289.4(5)	174(6)	3443	2609	303.1
	OW3	H31	O1	291.7(4)	152(6)	3502	2638	311.9
	OW3	H32	O4	279.3(3)	160(6)		2523	286.2
	O1	H1	O2	271.3(4)	167(7)		2273	261.4
	O2	H2	O3	265.5(4)	158(6)		2244	259.5
Ni	OW1	H11	O3	281.7(3)	156(4)		2568	293.9
	OW1	H12	O4	264.3(3)	175(4)	2927	2429	274.5
	OW2	H21	O3	276.0(3)	164(5)		sh.	
	OW2	H22	OW1	289.4(4)	174(4)	3428	2592	299.0
	OW3	H31	O1	288.4(3)	155(5)	3481	n.o.	
	OW3	H32	O4	279.2(3)	160(6)		2512	284.6
	O1	H1	O2	270.0(3)	164(6)		2449	276.6
	O2	H2	O3	265.9(3)	170(5)		2201	256.9
Zn	OW1	H11	O3	280.6(3)	160(4)		2576	295.5
	OW1	H12	O4	264.5(3)	174(5)	2923	2432	274.8
	OW2	H21	O3	277.6(3)	165(5)		2504	283.4
	OW2	H22	OW1	288.2(4)	169(5)	3370	2593	299.2
	OW3	H31	O1	290.0(4)	156(5)	3483	2661	321.1
	OW3	H32	O4	280.4(3)	164(6)		2519	285.6
	O1	H1	O2	270.9(4)	164(6)		2391	270.7
	O2	H2	O3	266.1(3)	176(6)		2269	261.2

Table 4. Hydrogen bond lengths  $r_{DA}$  (pm) and angles  $\langle DHA \rangle$  (deg) in  $ZnH_4I_2O_{10} \cdot 6H_2O$ ,  $NiH_4I_2O_{10} \cdot 6H_2O$ , and  $MgH_4I_2O_{10} \cdot 6H_2O$ , their assignment to the IR absorption peaks  $\nu(OH)$  and  $\nu(OD)$  ( $cm^{-1}$ ) and O...O distances  $r_{DA}(\text{calcd.})$  (pm) calculated from the decoupled OD stretching vibrations according to Mikenda [7].

Decomposition reaction	$T$ ( $^{\circ}C$ )	$\Delta m_{\text{exp}}$ (%)	$\Delta m_{\text{theor}}$ (%)
$ZnH_4I_2O_{10} \cdot 6H_2O \rightarrow Zn(H_4IO_6)_2 \cdot H_2O + 3H_2O$	80–120	9.5	9.1
$Zn(H_4IO_6)_2 \cdot H_2O \rightarrow Zn(IO_4)_2 \cdot 2H_2O + 3H_2O$	130–170	18.3	18.3
$Zn(IO_4)_2 \cdot 2H_2O \rightarrow Zn(IO_3)_2 + 2H_2O + O_2$	> 170	29.1	29.8

Table 5. Scheme of the thermal decomposition of  $ZnH_4I_2O_{10} \cdot 6H_2O$ .

$h$	$k$	$l$	int.	$d(\text{obs.})$	$d(\text{calcd.})$	$h$	$k$	$l$	int.	$d(\text{obs.})$	$d(\text{calcd.})$
0	4	0	42.8	8.4127	8.4363	3	9	1	19.2	2.7747	2.7787
0	2	1	82.4	5.1896	5.1969	6	0	1	18.8	2.7431	2.7421
2	6	0	46.4	4.8299	4.8412	7	1	0	18.8	2.7064	2.7088
1	3	1	47.9	4.7562	4.7576	0	4	2	32.2	2.5988	2.5985
0	4	1	100.0	4.5826	4.5852	6	9	0	18.4	2.4196	2.4210
1	4	1	79.1	4.4656	4.4576	11	4	0	17.5	2.2893	2.3912
0	5	1	50.1	4.2451	4.2460	0	14	1	17.5	2.2642	2.2054
1	5	1	48.9	4.1351	4.1440	2	16	0	16.5	2.2030	2.0591
3	2	1	35.6	4.0125	4.0195	9	4	0	17.2	2.0482	2.0503
1	6	1	48.5	3.8432	3.8379	8	7	1	16.4	1.9878	1.9865
1	9	0	48.7	3.6795	3.6787	7	1	2	14.6	1.9219	1.9233
2	9	0	34.9	3.4871	3.4882	9	10	0	9.0	1.7915	1.7913
5	0	1	42.8	3.1225	3.1220	1	6	3	13.0	1.7254	1.7252
2	9	1	24.5	2.9392	2.9399	11	6	0	16.8	1.6517	1.6517
0	10	1	31.9	2.8697	2.8709	5	3	3	12.6	1.6257	1.6257
1	10	1	20.7	2.8387	2.8387	10	10	3	11.6	1.4160	1.4160

Table 6. Powder diffraction data of a  $ZnH_4I_2O_{10} \cdot 6H_2O$  sample decomposed at  $80^{\circ}C$  (orthorhombic,  $a = 1902.6$ ,  $b = 3376.0$  and  $c = 546.1$  pm).

by the correlation of Mikenda [7]. This assignment is complicated by the fact that according to the *ab initio* calculation [6] the OH stretching vibrations of the acidic protons of the periodate ions are expected within the same wavenumber range as the OD stretching vibrations of HDO molecules. As can be seen from Table 4 the distances of oxygen atoms coupled *via* hydrogen bridges are between 290 and 260 pm.

#### Thermochemistry of $ZnH_4I_2O_{10} \cdot 6H_2O$

The thermal decomposition of  $ZnH_4I_2O_{10} \cdot 6H_2O$  was studied by differential thermal analysis (DTA) and thermogravimetric analysis (TG) in the temperature range  $25-475^{\circ}C$  (Fig. 7) as well as by high-temperature Raman spectroscopy (Fig. 8). A scheme for the thermal decomposition of  $ZnH_4I_2O_{10} \cdot 6H_2O$ ,

<i>h</i>	<i>k</i>	<i>l</i>	int.	<i>d</i> (obs.)	<i>d</i> (calcd.)	<i>h</i>	<i>k</i>	<i>l</i>	int.	<i>d</i> (obs.)	<i>d</i> (calcd.)
1	1	1	11.3	5.4769	5.4641	-5	0	5	7.4	2.2566	2.2582
0	2	0	12.7	4.7386	4.7293	0	4	2	11.1	2.1471	2.1479
0	1	2	10.8	4.5111	4.5128	1	5	0	20.0	1.8719	1.8731
-3	1	2	8.6	4.2266	4.2230	2	4	3	3.2	1.7396	1.7408
-4	0	1	9.2	3.7758	3.7766	-1	2	6	7.9	1.6933	1.6946
0	2	2	100.0	3.4806	3.4787	-2	0	7	6.7	1.6091	1.6102
-3	0	4	6.2	2.9409	2.9456	-2	1	7	2.8	1.5862	1.5874
3	2	1	5.3	2.8158	2.8140	4	2	4	4.5	1.5768	1.5776
0	3	2	4.4	2.6863	2.6868	-1	3	7	3.2	1.3866	1.3866
0	0	4	12.2	2.5671	2.5674	2	6	3	2.8	1.3435	1.3441
-3	3	3	4.2	2.4158	2.4169	-11	2	1	2.7	1.2377	1.2384
-6	1	1	3.3	2.3636	2.3650						

Table 7. Powder diffraction data of a  $\text{ZnH}_4\text{I}_2\text{O}_{10}\cdot 6\text{H}_2\text{O}$  sample decomposed at 150 °C (monoclinic,  $a = 1776.2$ ,  $b = 493.1$ ,  $c = 942.9$  pm,  $\beta = 101.72^\circ$ ).

which is in accord with the experimental data, is shown in Table 5.

As the thermal analysis and the high-temperature Raman spectra show (Figs. 7 and 8),  $\text{ZnH}_4\text{I}_2\text{O}_{10}\cdot 6\text{H}_2\text{O}$  is stable up to  $\sim 75$  °C. The DTA diagram exhibits an endothermic effect at 80 °C which is probably due to a conversion of the tetrahydrogendecaoxidiperiodate to the monoperiodate  $\text{Zn}(\text{H}_4\text{IO}_6)_2\cdot 4\text{H}_2\text{O}$ . This is supported by the great similarity of the Raman spectrum of this compound to the spectrum of  $\text{Be}(\text{H}_4\text{IO}_6)_2\cdot 4\text{H}_2\text{O}$  published by Maneva *et al.* [8]. The X-ray powder data of a sample decomposed at 80 °C compiled in Table 6 can be fully indexed on the basis of an orthorhombic unit cell with  $a = 1902.6$ ,  $b = 3376.0$  and  $c = 546.1$  pm.

At temperatures up to 120 °C the monoperiodate  $\text{Zn}(\text{H}_4\text{IO}_6)_2\cdot 4\text{H}_2\text{O}$  loses 3 moles of  $\text{H}_2\text{O}$  (mass loss: found 9.49 %, calcd. 9.13 %) forming the monohydrate  $\text{Zn}(\text{H}_4\text{IO}_6)_2\cdot \text{H}_2\text{O}$ .

The compound formed in the temperature interval 130–170 °C could not be identified by Raman spectroscopy beyond doubt. Presumably this material is a hitherto unknown metaperiodate  $\text{Zn}(\text{IO}_4)_2\cdot 2\text{H}_2\text{O}$ . The calculated mass loss of 18.27 % for 3 moles of water is in good accordance with the experimental value of 18.3 %. The X-ray powder data for a sample decomposed at 150 °C (Table 7) can be indexed in the monoclinic system with the lattice parameters  $a = 1776.2$ ,  $b = 493.1$ ,  $c = 942.9$  pm and  $\beta = 101.72^\circ$ .

The exothermic peak at 170 °C accompanied by a mass loss of 29.1 % is due to the formation of zinc iodate  $\text{Zn}(\text{IO}_3)_2$ . The calculated mass loss for 2 moles of  $\text{H}_2\text{O}$  and 1 mole of  $\text{O}_2$  is 29.7 %. In the Raman spectrum of this product the vibrations characteristic for iodates are observed in the region 810–730  $\text{cm}^{-1}$ . The powder diffraction diagram of a sample decomposed at 300 °C is in good accordance with the data calculated on the basis of the structural data for  $\text{Zn}(\text{IO}_3)_2$  given by Liang and Wang [9].

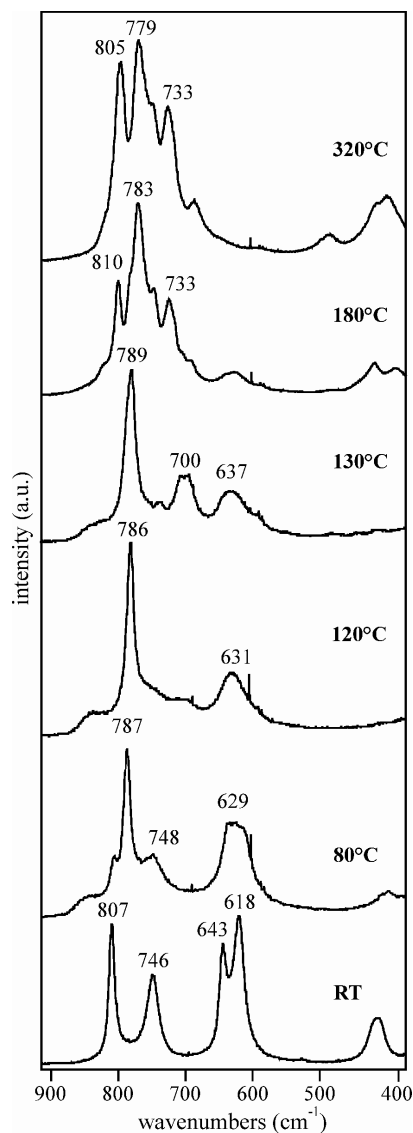


Fig. 8. High-temperature Raman spectra of  $\text{ZnH}_4\text{I}_2\text{O}_{10}\cdot 6\text{H}_2\text{O}$ .

### Thermochemistry of $\text{NiH}_4\text{I}_2\text{O}_{10} \cdot 6\text{H}_2\text{O}$

$\text{NiH}_4\text{I}_2\text{O}_{10} \cdot 6\text{H}_2\text{O}$  already decomposes in the laser beam during the measurement of the Raman spectra if the laser power is  $> 20$  mW. Therefore high-temperature Raman spectra of this compound could not be obtained, but the spectra produced with variable power of the laser (Fig. 9) also give some insight in the thermal decomposition process of the Ni salt. The decomposition of the substance which starts at about 20 mW is due to a warming of the sample in the focus of the laser beam leading to dehydration and a transformation. This reaction is nearly complete at a laser power of 40 mW. The spectrum obtained at this laser power shows an intense peak at  $798\text{ cm}^{-1}$  pointing to the formation of a metaperiodate as the decomposition product.

Results of the DTA and TG measurements on  $\text{NiH}_4\text{I}_2\text{O}_{10} \cdot 6\text{H}_2\text{O}$  are shown in Fig. 10. A scheme for the

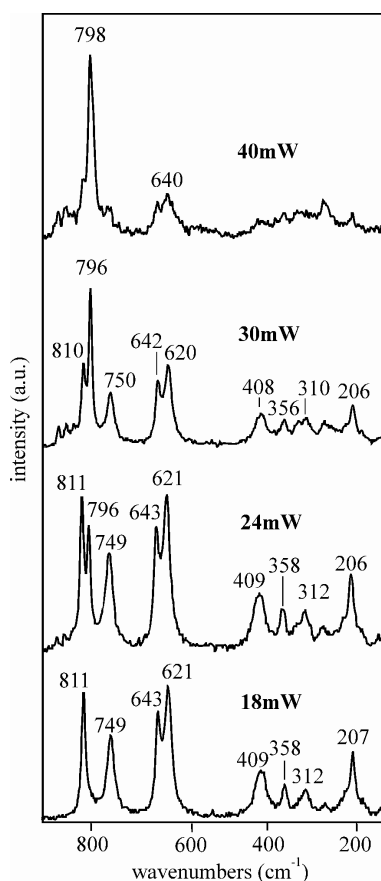


Fig. 9. Raman spectra of  $\text{NiH}_4\text{I}_2\text{O}_{10} \cdot 6\text{H}_2\text{O}$  measured with different laser power.

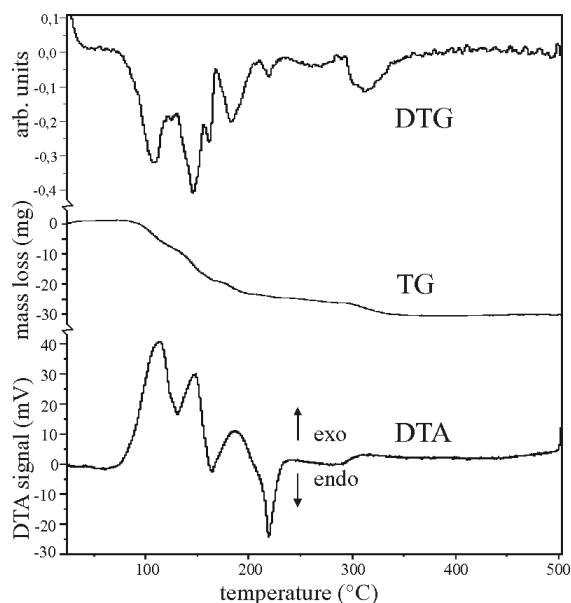


Fig. 10. Differential thermal analysis (DTA), thermogravimetric analysis (TG) and differential TG (DTG) of  $\text{NiH}_4\text{I}_2\text{O}_{10} \cdot 6\text{H}_2\text{O}$ .

thermal decomposition of  $\text{NiH}_4\text{I}_2\text{O}_{10} \cdot 6\text{H}_2\text{O}$ , which is in accordance with the experimental data, is shown in Table 8.

According to the thermal analysis (Fig. 10) the dehydration of  $\text{Ni}(\text{H}_4\text{IO}_6)_2 \cdot 4\text{H}_2\text{O}$  starts at  $80^\circ\text{C}$  with an endothermic reaction accompanied by the loss of 2 moles of water. The shoulder which can be observed on the corresponding peak (Fig. 10) points to a two-step reaction for this process. For the first step we assume – in analogy to the decomposition of  $\text{Zn}(\text{H}_4\text{IO}_6)_2 \cdot 4\text{H}_2\text{O}$  (s. above) – a change from the diperiodate to a monoperoiodate. This assumption is supported by a comparison of the Raman spectrum of  $\text{Zn}(\text{H}_4\text{IO}_6)_2 \cdot 4\text{H}_2\text{O}$  measured at  $120^\circ\text{C}$  (Fig. 7) and that of the product of the decomposition of  $\text{Ni}(\text{H}_4\text{IO}_6)_2 \cdot 4\text{H}_2\text{O}$  in the laser light (Fig. 10, 40 mW). Both spectra show a great similarity in the region of the internal vibrations of the periodate ions.

The tetrahydrogenhexaoxoperiodate loses again 2 moles of water and undergoes a transformation to the metaperiodate  $\text{Ni}(\text{IO}_4)_2 \cdot 2\text{H}_2\text{O}$  in the temperature range  $130\text{--}160^\circ\text{C}$  in a two-step process.

The exothermic reaction at  $165^\circ\text{C}$  is accompanied by a mass loss of about 2.5 % due to a partial reduction of the periodate by splitting off  $1/2$  mole  $\text{O}_2$  ( $\Delta m_{\text{theor}}$ : 2.75 %). This is in agreement with the formation of a sample with the composition  $\text{Ni}(\text{I}_2\text{O}_7) \cdot 2\text{H}_2\text{O}$ . The

Decomposition reaction	<i>T</i> (°C)	$\Delta m_{\text{exp}}$ (%)	$\Delta m_{\text{theor}}$ (%)
$\text{NiH}_4\text{I}_2\text{O}_{10} \cdot 6\text{H}_2\text{O} \rightarrow \text{Ni}(\text{H}_4\text{IO}_6)_2 \cdot 2\text{H}_2\text{O} + 2\text{H}_2\text{O}$	80–120	6.5	6.2
$\text{Ni}(\text{H}_4\text{IO}_6)_2 \cdot 2\text{H}_2\text{O} \rightarrow \text{Ni}(\text{IO}_4)_2 \cdot 2\text{H}_2\text{O} + 2\text{H}_2\text{O}$	130–170	12.5	12.3
$\text{Ni}(\text{IO}_4)_2 \cdot 2\text{H}_2\text{O} \rightarrow \text{Ni}(\text{I}_2\text{O}_7) \cdot 2\text{H}_2\text{O} + 1/2 \text{O}_2$	> 170	2.0	2.8
$\text{Ni}(\text{I}_2\text{O}_7) \cdot 2\text{H}_2\text{O} \rightarrow \text{Ni}(\text{I}_2\text{O}_7) + 2\text{H}_2\text{O}$	180	5.5	6.2
$\text{Ni}(\text{I}_2\text{O}_7) \rightarrow \text{Ni}(\text{IO}_3)_2 + 1/2 \text{O}_2$	220	2.0	2.8

Table 8. Scheme of the thermal decomposition of  $\text{NiH}_4\text{I}_2\text{O}_{10} \cdot 6\text{H}_2\text{O}$ .

decision whether this is a mixed iodate-periodate of nickel or a salt of a mixed valent acid of iodine ( $\text{I}_2\text{O}_7^{2-}$  or  $\text{H}_4\text{I}_2\text{O}_9^{2-}$ ) cannot be made on the basis of the existing experimental data and needs further investigation.

The last 2 moles of water are split off in another exothermic process at 180 °C shortly before at 220 °C the anhydrous iodate  $\text{Ni}(\text{IO}_3)_2$  is formed by loss of another 1/2 mole of oxygen. As can be seen from powder X-ray diffraction data, the final product of the thermal decomposition of  $\text{NiH}_4\text{I}_2\text{O}_{10} \cdot 6\text{H}_2\text{O}$  is  $\text{NiO}$  at 600 °C.

### Experimental Section

The products of the thermal decomposition of the Ni and Zn periodates have been characterized by X-ray powder diffraction using a Siemens powder diffractometer D5000 equipped with a primary monochromator and a position-sensitive detector PSD-50M (Braun GmbH) with  $\text{CuK}\alpha_1$  ( $\lambda = 154.05$  pm) radiation. The calculation of the lattice parameters was done with the program package VISUAL X<sup>POW</sup>.

The infrared spectra of the compounds were measured at r.t. on powdered samples with a Bruker FTIR spectrometer IFS 113v using Nujol and polychlorotrifluoroethylene mulls on  $\text{CaF}_2$  or polyethylene windows and with a Bruker FTIR spectrometer Tensor 27 using a MIRacle ATR unit. KBr, CsI or NaCl windows cannot be used because of their reaction with the periodate. As a consequence the measuring range was restricted to  $> 1000$   $\text{cm}^{-1}$ . The Raman spectra were recorded with the laser Raman spectrograph Dilor Omars 89 in 90° measuring geometry with an excitation wavelength of 514.5 nm, and in 180° measuring geometry with a Bruker Raman spectrometer RFS 100/S with an excitation wavelength of 1064 nm of a Nd:YAG laser. For the Raman measurements at low temperatures a Bruker Raman low temperature cell R 495 was used. The resolution of all vibrational spectra was fixed to 2  $\text{cm}^{-1}$ .

Simultaneous differential thermal (DTA) and thermogravimetric (TG) investigations have been made in the temperature range from r.t. to 600 °C using a heating rate of 10 °C/min with a Linseis thermobalance L81 on 30–70 mg samples.  $\text{Al}_2\text{O}_3$  was used as a reference.

#### *NiH<sub>4</sub>I<sub>2</sub>O<sub>10</sub>·6H<sub>2</sub>O*

Crystals of  $\text{NiH}_4\text{I}_2\text{O}_{10} \cdot 6\text{H}_2\text{O}$  were prepared from a concentrated aqueous solution of 0.2 g  $\text{NiCO}_3 \cdot \text{Ni}(\text{OH})_2$  (p. a., Merck) and 4.0 g periodic acid  $\text{H}_5\text{IO}_6$  (p. a., Merck) in 10 mL of water at r. t. The solution which had a pH of about 1 was stirred for 10 min, filtered and then stored in a desiccator over silica gel. After 3 weeks green crystals were formed which were soluble in water.

#### *ZnH<sub>4</sub>I<sub>2</sub>O<sub>10</sub>·6H<sub>2</sub>O*

Well crystallized  $\text{ZnH}_4\text{I}_2\text{O}_{10} \cdot 6\text{H}_2\text{O}$  was prepared from a solution of 4 g  $\text{H}_5\text{IO}_6$  (p. a., Merck) and 0.2 g  $\text{Zn}(\text{CO}_3)_2 \cdot \text{Zn}(\text{OH})_2$  (p. a., Merck) in 10 mL of water. From the clear solution which had a pH < 1, colorless crystals were obtained after about 4 weeks. The crystals were separated from the solution by filtration, dried with filter paper and stored in a desiccator over silica gel.

#### *MgH<sub>4</sub>I<sub>2</sub>O<sub>10</sub>·6H<sub>2</sub>O*

Crystals of  $\text{MgH}_4\text{I}_2\text{O}_{10} \cdot 6\text{H}_2\text{O}$  were prepared according to the method given in the literature [2].

#### *X-Ray structure determination*

For the structure determinations single crystals with dimensions given in Table 1 for the three compounds were selected. Intensity data were collected at r.t. on a Stoe IPS diffractometer ( $\text{MoK}\alpha$ ,  $\lambda = 0.7107$  Å, graphite monochromator) for  $3 \leq 2\theta \leq 31^\circ$ . Absorption correction was done empirically by the program X-SHAPE. Calculations were performed with the structure determination package SHELXS/L97. A summary of the conditions of the crystal structure determination and some crystallographic data are given in Table 1.

Further details of the crystal structure investigation may be obtained from Fachinformationszentrum Karlsruhe, D-76344 Eggenstein-Leopoldshafen, Germany (fax: (+49) 7247-808-666; e-mail: crysdata@fiz-karlsruhe.de, [http://www.fiz-karlsruhe.de/request\\_for\\_deposited\\_data.html](http://www.fiz-karlsruhe.de/request_for_deposited_data.html)) on quoting CSD 419502 (Ni compound), CSD 419504 (Zn compound) and CSD 419503 (Mg compound).

#### *Acknowledgements*

We thank Prof. Mormann, Univ. Siegen for the IR measurements with the MIRacle ATR unit. M. A. is grateful to the DAAD for financial support during her PhD studies.

- [1] M. Jansen, R. Müller, *Z. Anorg. Allg. Chem.* **1996**, 622, 1901 – 1906.
- [2] R. Nagel, M. Botova, G. Pracht, E. Suchanek, M. Maneva, H. D. Lutz, *Z. Naturforsch.* **1999**, 54b, 999 – 1008.
- [3] Z. Zhang, E. Suchanek, D. Eßer, M. Maneva, D. Nikolova, H. D. Lutz, *Z. Anorg. Allg. Chem.* **1996**, 622, 845 – 852.
- [4] M. A. Nabar, V. D. Athawale, *Thermochim. Acta* **1986**, 97, 85 – 91.
- [5] M. Botova, R. Nagel, H. Haeuseler, *Z. Anorg. Allg. Chem.* **2004**, 630, 179 – 184.
- [6] R. Jaquet, H. Haeuseler, *J. Raman Spectrosc.* **2008**, 39, 599 – 506.
- [7] W. Mikenda, *J. Mol. Struct.* **1986**, 147, 1 – 15.
- [8] M. Maneva, M. Georgiev, N. Lange, H. D. Lutz, *Z. Naturforsch.* **1991**, 46b, 795 – 799.
- [9] Liang Jinkui, Wang Chaoguo, *Acta Chimica Sinica* **1982**, 40, 985 – 993.